CANCER

Development of a prosaposin-derived therapeutic cyclic peptide that targets ovarian cancer via the tumor microenvironment

Suming Wang,[1,2]* Anna Blois,[1,2,3]* Tina El Rayes,[4,5,6]* Joyce F. Liu,[7,8] Michelle S. Hirsch,[9] Karsten Gravdal,[3,10] Sangeetha Palakurthi,[11] Diane R. Bielenberg,[1,2] Lars A. Akslen,[3,10] Ronny Drapkin,[8,9†] Vivek Mittal,[4,5,6] Randolph S. Watnick[1,2‡]

The vast majority of ovarian cancer–related deaths are caused by metastatic dissemination of tumor cells, resulting in subsequent organ failure. However, despite our increased understanding of the physiological processes involved in tumor metastasis, there are no clinically approved drugs that have made a major impact in increasing the overall survival of patients with advanced, metastatic ovarian cancer. We identified prosaposin (psap) as a potent inhibitor of tumor metastasis, which acts via stimulation of p53 and the antitumorigenic protein thrombospondin-1 (TSP-1) in bone marrow–derived cells that are recruited to metastatic sites. We report that more than 97% of human serous ovarian tumors tested express CD36, the receptor that mediates the proapoptotic activity of TSP-1. Accordingly, we sought to determine whether a peptide derived from psap would be effective in treating this form of ovarian cancer. To that end, we developed a cyclic peptide with drug-like properties derived from the active sequence in psap. The cyclic psap peptide promoted tumor regression in a patient-derived tumor xenograft model of metastatic ovarian cancer. Thus, we hypothesize that a therapeutic agent based on this psap peptide would have efficacy in treating patients with metastatic ovarian cancer.

INTRODUCTION

Ovarian cancer is the most lethal gynecologic malignancy and the fourth leading cause of cancer deaths in women (*1*). Pathologically, ovarian cancer is categorized into multiple subtypes, with epithelial-derived tumors being the predominant and most lethal form (*1*, *2*). Within this group, the serous ovarian subtype is the most prevalent (*1*, *2*). Despite our increased understanding of the biology governing the progression of epithelial ovarian cancer (EOC) and, more specifically, high-grade serous ovarian cancer (HGSOC), the survival rate for patients with advanced-stage disease remains low (*1*, *3*). Hence, there is a compelling need for therapies that can effectively treat advanced, metastatic ovarian cancer. Although many ovarian cancer patients display a transient response to platinum agents when these are used as first-line therapy, the vast majority develop recurrent chemoresistant disease within 6 to 18 months (*4*, *5*). Currently, there are no approved therapies that meaningfully increase overall survival for these patients.

We previously reported that prosaposin (psap) potently inhibits tumor metastasis in multiple tumor models (*6*, *7*). Specifically, we determined that psap, and a five–amino acid peptide residing within it, inhibits tumor metastasis by stimulating the production and release of the antitumorigenic protein thrombospondin-1 (TSP-1) (*8*–*10*) by $CD11b^{+}/GR1^{+}/Lys6C^{hi}$ monocytes (*6*). These monocytes are recruited to sites of future metastatic lesions, termed premetastatic niches, where they persist after colonization and stimulate tumor growth (*11*). Systemic administration of the psap peptide stimulates the production of TSP-1 in these cells, which renders the sites to which they are recruited refractory to future metastatic colonization (*6*). These results demonstrated that stimulation of TSP-1 in the tumor microenvironment could repress the formation of subsequent metastatic colonies. Unfortunately, as many as 75% of ovarian cancer patients present with metastatic disease at initial diagnosis (*1*). Hence, a therapeutic agent that could shrink, or at least stabilize, metastatic lesions is desperately needed.

Here, we demonstrate that stimulating TSP-1 in the microenvironment of a metastatic, platinum-resistant, ovarian cancer patient-derived xenograft (PDX) model can induce regression of established lesions. We show that this striking effect is achieved because of the fact that HGSOC cells express the receptor for TSP-1, CD36. CD36 mediates a proapoptotic effect in ovarian tumor cells that, until recently, was observed primarily in endothelial cells (*12*, *13*). Thus, our findings represent a potential therapeutic strategy for metastatic ovarian cancer.

RESULTS

Incorporation of D-amino acids increases the activity of a psap peptide in vivo

We previously described the identification of four– and five–amino acid peptides derived from the saposin A domain of psap that, when administered systemically, were able to inhibit the formation of metastases in a tail vein model of Lewis lung carcinoma and in an adjuvant model of human breast cancer metastasis (*6*). Although these findings were encouraging, the therapeutic efficacy of linear peptides

[1]Vascular Biology Program, Boston Children's Hospital, Boston, MA 02115, USA. [2]Department of Surgery, Harvard Medical School, Boston, MA 02115, USA. [3]Centre for Cancer Biomarkers (CCBIO), Department of Clinical Medicine, University of Bergen, NO-5020 Bergen, Norway. [4]Department of Cardiothoracic Surgery, Weill Cornell Medical College, New York, NY 10065, USA. [5]Department of Cell and Developmental Biology, Weill Cornell Medical College, New York, NY 10065, USA. [6]Neuberger Berman Lung Cancer Center, Weill Cornell Medical College, New York, NY 10065, USA. [7]Department of Medicine, Harvard Medical School, Boston, MA 02115, USA. [8]Department of Medical Oncology, Dana-Farber Cancer Institute, Boston, MA 02115, USA. [9]Department of Pathology, Harvard Medical School, Boston, MA 02115, USA. [10]Department of Pathology, Haukeland University Hospital, N-5021 Bergen, Norway. [11]Belfer Center for Applied Cancer Science, Dana-Farber Cancer Institute, Boston, MA 02115, USA.
*These authors contributed equally to this work.
†Present address: Department of Obstetrics and Gynecology, Ovarian Cancer Research Center, University of Pennsylvania, Philadelphia, PA 19104, USA.
‡Corresponding author. E-mail: randy.watnick@childrens.harvard.edu

is often limited by their instability. One common method of increasing the stability of peptides in vivo is to incorporate D-amino acids into the sequence, because D-amino acids are not incorporated into naturally occurring proteins and proteases do not recognize them as substrates (*14*–*18*). Hence, we sought to improve the stability of the four–amino acid psap peptide by incorporating D-amino acids at different residues. Specifically, we synthesized two peptides with D-amino acids incorporated, in combination, at the first (aspartate) and third (leucine), or at the second (tryptophan) and fourth (proline), residues. We tested the activity of these peptides along with the native L-amino acid peptide in vitro by measuring their ability to stimulate TSP-1 in WI-38 lung fibroblasts. We found, by Western blot analysis, that there was no difference in the amount of TSP-1 expression stimulated in these fibroblasts by the three peptides in vitro (Fig. 1A).

We then tested the activity of the 1,3-D-amino acid psap peptide and the native psap peptide in vivo. We systemically administered the peptides to C57BL6/J mice that were pretreated with conditioned medium (CM) from PC3M-LN4 (LN4) cells, which can mimic the systemic properties of metastatic tumors by repressing the expression of TSP-1 in the lungs of mice (*6*, *7*). After 3 days of treatment with LN4 CM alone or in combination with the D- or L-amino acid peptides at a dose of 30 mg/kg, we prepared proteins pooled from the harvested lungs of each treatment group. We then quantified TSP-1 expression in the lungs of these mice by Western blot analysis. We observed that the 1,3-D-amino acid peptide stimulated TSP-1 expression more than 10-fold greater than the native peptide (Fig. 1B). In light of the observation that the in vitro activity of the two peptides was virtually identical, we surmised that the difference in activity in vivo was due to a difference in stability in the circulation.

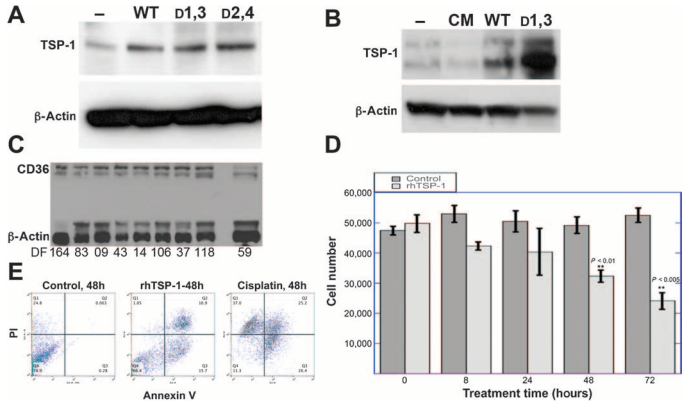

Fig. 1. Stimulation of TSP-1 and its effects on ovarian cancer cell growth and survival. (**A**) Western blot of TSP-1 and β-actin in WI-38 lung fibroblasts that were untreated (–) or treated with the native DWLP L-amino acid psap peptide [wild type (WT)], dWlP psap peptide (D1,3), or DwLp psap peptide (D2,4) ($n = 5$). (**B**) Western blot of TSP-1 and β-actin in pooled mouse lung tissue harvested from mice that were untreated (–) or treated with metastatic prostate cancer cell CM alone (CM) or in combination with DWLP psap peptide (WT) or dWlP psap peptide (D1,3 peptide) at doses of 30 mg/kg per day intraperitoneally for 3 days ($n = 3$ mice per group). (**C**) Western blot of CD36 and β-actin in nine patient-derived ovarian cancer cell lines (DF). (**D**) Plot of cell number as measured by Wst-1 assay of patient-derived ovarian cancer cell line DF14 treated with 0.2 nM rhTSP-1 for 8, 24, 48, or 72 hours [*P* values were calculated by analysis of variance (ANOVA)] ($n = 3$) (error bars indicate SEM). (**E**) FACS analysis of annexin V and PI staining in patient-derived ovarian cancer cell line DF14 treated with saline (control, left), 0.2 nM rhTSP-1 (middle), and cisplatin (10 μg/ml) (right) for 48 hours (cells staining positive for both markers are apoptotic) ($n = 3$).

Human HGSOC cells are sensitive to killing by TSP-1

To test the efficacy of the D-amino acid psap peptide, we sought to determine a suitable tumor model that would represent a potential clinical application for the peptide. Given that psap, and the peptide we derived from it, stimulates TSP-1 protein expression in bone marrow–derived cells that are recruited to sites of metastasis, we sought to identify a specific type of cancer that expresses CD36, the receptor for TSP-1 that mediates its proapoptotic activity (*12*). Serous ovarian epithelial cells and human ovarian cancer cells express CD36 (*13*, *19*, *20*). Accordingly, we surveyed 12 primary human ovarian cancer cell lines derived from the ascites of patients with HGSOC for the expression of CD36. We found that all 12 of the patient-derived cell lines tested expressed CD36, which was readily detectable by Western blot (Fig. 1C and fig. S1). We then treated three of these cell lines (DF14, DF118, and DF216) (table S1) with recombinant human TSP-1 (rhTSP-1) (0.2 nM) for up to 72 hours in vitro and determined its effect on cell number [as measured via water-soluble tetrazolium salt 1 (Wst-1)] and apoptosis. We found that rhTSP-1 treatment reduced cell numbers by up to 50% after 72 hours (Fig. 1D; $P = 0.0094$ at 48 hours and 0.0014 at 72 hours by Student's *t* test). Moreover, we observed by fluorescence-activated cell sorting (FACS) analysis that 30 to 60% of TSP-1–treated cells in all three patient-derived cell lines were undergoing apoptosis after TSP-1 treatment, as defined by annexin V positivity (Fig. 1E and fig. S2). In contrast, we observed that, after cisplatin treatment, a much greater percentage of ovarian cancer cells underwent necrosis, as defined by low annexin V and high propidium iodide (PI) staining (Fig. 1E). Finally, we treated the DF14 patient-derived cell line with rhTSP-1 in combination with an antibody to CD36 that blocks TSP-1 binding (*21*). We found that the percentage of cells in late apoptosis, defined as staining positive for PI and annexin V, increased from 8.44 to 18.1% when the cells were treated with rhTSP-1 alone (compared to untreated cells) (fig. S3). Strikingly, when DF14 cells were treated with rhTSP-1 in combination with the CD36 antibody, the percentage of cells in late apoptosis decreased from 18.1 to 6.98% (fig. S3). These findings suggest that ovarian cancer cells may respond favorably to treatment with the psap peptide.

The psap peptide induces regression in primary ovarian tumors

We sought to determine whether the D1,3 psap peptide could be effective in treating primary ovarian tumors. Therefore, we made use of the murine 1D8 ovarian cancer cell line to test the activity of the psap peptide in a syngeneic model with an intact immune system (*22*). 1D8 cells also express CD36, the receptor for TSP-1 (*13*, *19*). We injected 1×10^6 luciferase-expressing 1D8 cells orthotopically into the ovarian bursa of immunocompetent C57BL6/J mice. We allowed the tumors to grow for 31 days before initiating treatment with saline or the D1,3 psap peptide at a dose of 40 mg/kg per day ($n = 8$ per group). At the time of treatment, the difference in the average luciferase intensity of the peptide and control groups was not statistically significant (3.76×10^6 versus 5.76×10^6; $P = 0.596$ by Mann-Whitney *U* test). We treated the mice with the psap peptide for 20 days, at which point the average luciferase intensity of the psap peptide–treated tumors was significantly lower than that of the control-treated tumors (3.32×10^6 versus 2.46×10^7; $P = 0.00438$ by Mann-Whitney *U* test) (Fig. 2A). We then discontinued treatment to determine whether the tumors would remain inhibited or grow out.

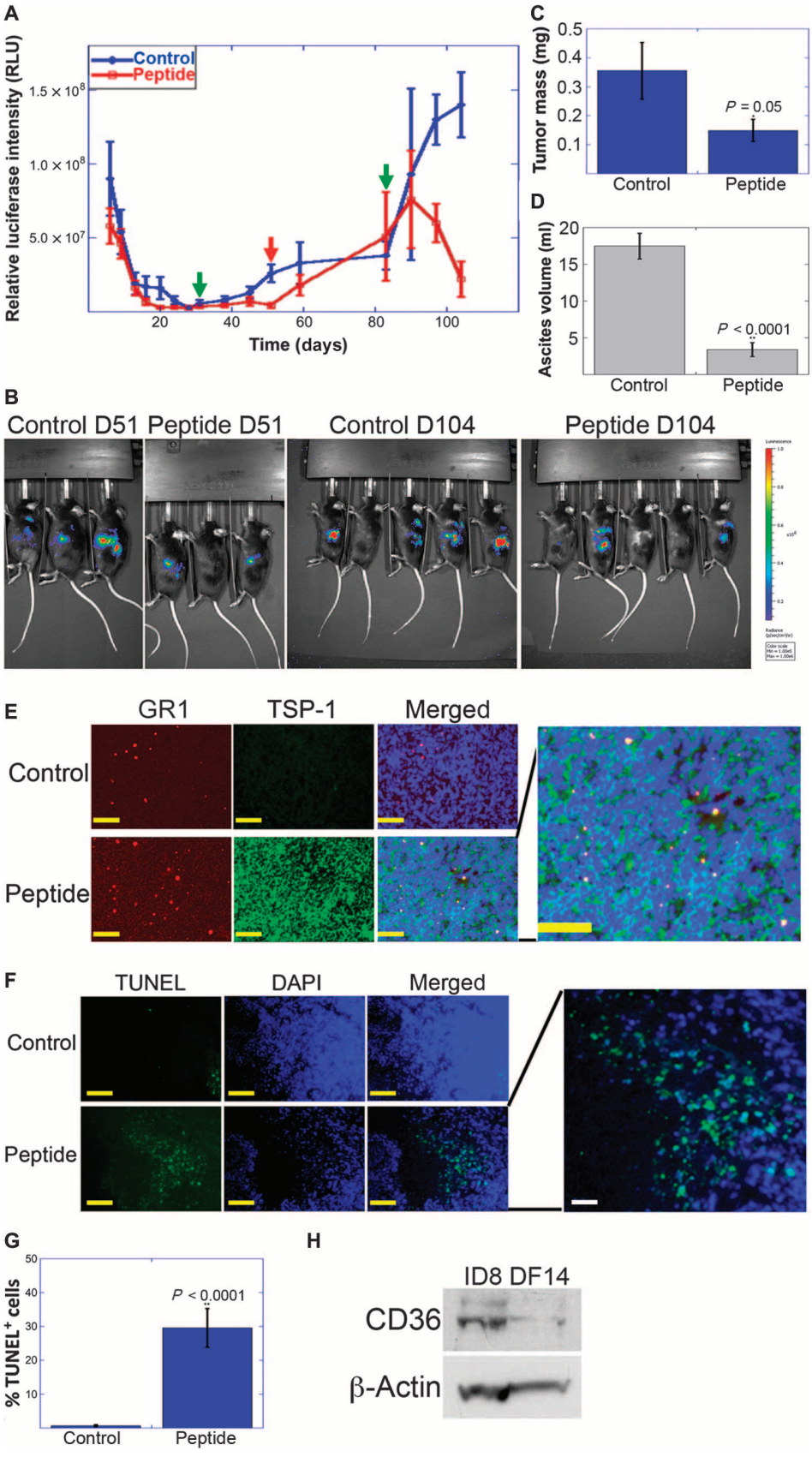

Fig. 2. Regression of primary ovarian tumors induced by the psap peptide. (**A**) Plot of luciferase intensity over time in 1D8 tumors treated with saline (Control) or psap peptide (Peptide). Mice were treated daily with dWlP peptide (40 mg/kg) on days 31 to 51 and 83 to 104 ($n = 8$ mice per group). Green arrows indicate initiation of treatment, and red arrow indicates cessation of treatment (mean ± SEM). (**B**) Images of luciferase intensity of 1D8 tumors in mice that were treated with saline (control) or psap peptide 51 and 104 days (D51 and D104) after injection ($n = 12$). (**C**) Plot of the average mass of 1D8 tumors at day 104 from mice that were treated with saline (Control) or psap peptide (Peptide) (mean ± SEM). (**D**) Plot of the average ascites volume of mice bearing 1D8 tumors that were treated with saline (Control) or psap peptide (Peptide) ($n = 8$) (mean ± SEM). (**E**) Immunofluorescence staining for GR1 (red), TSP-1 (green), and DAPI (4′,6-diamidino-2-phenylindole) (blue) in paraffin-embedded sections of 1D8 tumors treated with saline (Control) or psap peptide (Peptide) (yellow scale bars,100 μm; yellow scale bar in enlarged panel, 25 μm). (**F**) Immunofluorescence staining for TUNEL (green) and DAPI (blue) in paraffin-embedded sections of 1D8 tumors treated with saline (Control) or psap peptide (Peptide) (yellow scale bars, 100 μm; white scale bar, 25 μm). (**G**) Plot of average percentage of TUNEL$^+$ cells in 1D8 tumors treated with saline (Control) or psap peptide (Peptide) (mean ± SEM). (**H**) Western blot of CD36 and β-actin expression in 1D8 and DF14 cells.

After the cessation of treatment, we observed that not only did the tumors previously treated with psap peptide resume growing but also the average luciferase intensity was not significantly different than that of the control-treated tumors by day 83 (peptide, 5.03×10^7 versus 3.81×10^7; $P = 0.497$ by Mann-Whitney U test). Accordingly, the treatment was restarted at day 83 and continued for an additional 21 days. For the first week of treatment, the tumors continued to grow, though slower than the control-treated tumors (Fig. 2A). However, after the first week of treatment, the luciferase intensity of the psap peptide–treated tumors began to decrease, and after the third week of treatment (day 104), the average luciferase intensity of the psap peptide–treated group was lower than the intensity at day 83 and significantly lower than the control-treated group (1.17×10^7 versus 1.25×10^8; $P = 0.00578$ by Mann-Whitney U test) (Fig. 2, A and B). At this time, the control-treated mice began to show signs of morbidity, the experiment was ended, and the tumors were harvested, weighed, and analyzed histologically.

Upon gross examination of the mice, we made three striking observations. The first was that the peptide-treated tumors were about half the size (mass) of the control-treated tumors (51.2%; $P = 0.0086$ by Student's t test) (Fig. 2C). Second, consistent with human disease, the control-treated mice all developed severe ascites, whereas the psap peptide–treated mice had minimal to no ascites fluid (average ascites volume of 17.5 versus 3.4 ml per mouse; $P < 0.001$ by Student's t test; Fig. 2D). Third, when we examined the tumors histologically by immunofluorescence, we observed that the reduction in tumor size was accompanied by an induced expression of TSP-1 in $CD11b^+/GR1^+$ cells, as previously observed (*6*). We observed markedly increased TSP-1 expression in psap peptide–treated tumors compared to control-treated tumors and found that TSP-1 colocalized with $GR1^+$ cells (Fig. 2E). As demonstrated by TUNEL (terminal deoxynucleotidyl transferase–mediated deoxyuridine triphosphate nick end labeling) staining, psap peptide–treated 1D8 tumors contained, on average, 30% apoptotic cells, whereas control-treated 1D8 tumors contained less than 1% apoptotic cells (Fig. 2, F and G). These findings were consistent with the observation that 1D8 cells express even more CD36 than the patient-derived DF14 cells (Fig. 2H).

In addition to its ability to induce tumor cell apoptosis in a CD36-dependent manner, TSP-1 also has potent antiangiogenic activity via induction of endothelial cell apoptosis in a CD36-dependent manner (*12*). Accordingly, we analyzed the vascularity of 1D8 tumors to determine whether treatment with the psap peptide inhibited angiogenesis. We performed immunohistochemical analysis for CD31, a marker of endothelial cells, and observed a marked difference in vascularity between psap peptide–treated and control-treated tumors. Specifically, vessels in psap peptide–treated tumors occupied ~10-fold less area than those in the control-treated tumors (5.7% versus 0.59%; $P = 0.0011$ by Wilcoxon analysis) (Fig. 3, A and B). The vessels that were present in peptide-treated tumors were smaller than those in control tumors and did not appear to have open lumens (Fig. 3A, lower right panel). Moreover, psap peptide–treated tumors contained, on average, 4.3-fold fewer vessels than control-treated tumors (18.4 versus 4.3 vessels per field; $P = 0.004$ by Wilcoxon analysis) (Fig. 3, A and C).

In accordance with published reports that TSP-1 can stimulate the recruitment of macrophages (*23*), we sought to determine whether macrophage infiltration was affected by the stimulation of TSP-1 by the psap peptide. To do so, we stained tumor sections of psap peptide– and control-treated mice for CD107b (Mac-3) and found that psap peptide–treated tumors contained 8.5-fold more macrophages than control-treated tumors (80.0 versus 9.4; $P < 0.001$ by Wilcoxon analysis) (Fig. 3, D and E). This finding was consistent with the reported activity of TSP-1 in recruiting macrophages (*23*).

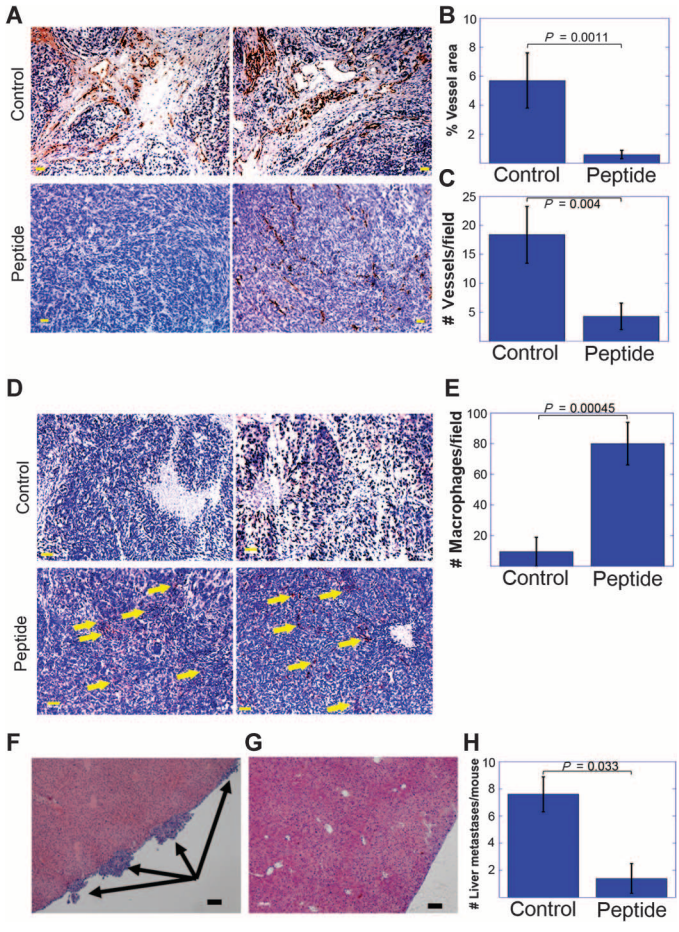

Fig. 3. Histological analysis of psap peptide–treated ovarian tumors. (**A**) Immunohistochemical analysis of CD31 staining to measure vascularity in saline (Control)– and D1,3 psap peptide (Peptide)–treated primary 1D8 ovarian tumors (scale bars, 100 μm). (**B**) Graphical depiction of vessel density (vessel area as a percentage of total field area) as determined by CD31 staining of saline (Control)– and D1,3 psap peptide (Peptide)–treated 1D8 tumors ($P = 0.0011$, Mann-Whitney U test). (**C**) Graphical depiction of vessel density (number of vessels per field) as determined by CD31 staining of saline (Control)– and D1,3 psap peptide (Peptide)–treated 1D8 tumors ($P = 0.004$, Mann-Whitney U test) (scale bars, 100 μm). (**D**) Immunohistochemical analysis of Mac3 staining to measure macrophage infiltration in saline (Control)– and D1,3 psap peptide (Peptide)–treated primary 1D8 ovarian tumors. Yellow arrows indicate Mac3-positive cells (scale bars, 100 μm). (**E**) Graphical depiction of macrophage infiltration, measured as the number of macrophages per field as determined by Mac3 staining of saline (Control)– and D1,3 psap peptide (Peptide)–treated 1D8 tumors ($P = 0.00328$, Mann-Whitney U test) ($n = 8$ mice per group). (**F**) H&E staining of liver surface implants (denoted by arrows) formed by 1D8 tumors in saline-treated mice (scale bar, 100 μm). (**G**) H&E staining of a representative liver of a mouse bearing a 1D8 tumor treated with D1,3 psap peptide (scale bar, 100 μm). (**H**) Graphical depiction of the number of liver metastases, both surface implants and parenchymal lesions in saline (Control)– and D1,3 psap peptide (Peptide)–treated mice bearing 1D8 tumors ($P = 0.033$, Mann-Whitney U test) ($n = 5$ mice per group).

Moreover, hematoxylin and eosin (H&E) examination of the livers of tumor-bearing mice revealed that five of five control-treated mice had extensive liver surface implant metastases (about eight metastases per liver), whereas the peptide-treated mice had significantly fewer metastases: three of five mice had no metastases, and of the remaining two mice, one had six and one had only one metastatic lesion ($P = 0.033$ by Wilcoxon analysis) (Fig. 3, F to H). On the basis of these findings, we conclude that the psap peptide is effective in treating primary ovarian tumors and inhibiting metastasis via three potential mechanisms: induction of tumor cell apoptosis, inhibition of angiogenesis, and promotion of macrophage infiltration.

The psap peptide induces regression in a PDX model of ovarian cancer

Although the ability of the psap peptide to shrink primary ovarian tumors and inhibit metastasis was an important proof of concept, unfortunately, 75% of ovarian cancer patients already have disseminated disease at the time of diagnosis (*1*). For these patients, inhibiting metastasis would have limited therapeutic benefit. Rather, these patients require a therapeutic agent that can shrink or, at the very least, stabilize existing metastases. Thus, we sought to determine whether the D-amino acid psap peptide could have therapeutic efficacy in a model of established metastatic dissemination. Accordingly, we injected 1×10^6 DF14 cells, which were isolated from the ascites of a patient with HGSOC, into the peritoneal cavity of severe combined immunodeficient (SCID) mice to mimic the route of dissemination of human ovarian cancer. This was one of the 12 PDX cell lines found to express CD36 (Fig. 1C and fig. S1) (*24*). The cells were retrovirally transduced with a vector expressing firefly luciferase, which allowed the growth of metastatic colonies in the mice to be monitored in real time via relative luciferase intensity. When the average intensity of the luciferase signal was 0.5×10^8 to 1×10^8 relative luciferase units (RLU), we began treatment with vehicle (saline) ($n = 12$), the D-amino acid peptide (40 mg/kg daily) ($n = 12$), or cisplatin (4 mg/kg every other day) ($n = 12$) (*25*). We observed that both the peptide and cisplatin decreased tumor volume, as determined by luciferase intensity, for the first 20 days of treatment (Fig. 4A). However, during those 20 days, half of the cisplatin-treated mice died from adverse side effects of the drug as defined by total body weight, which decreased by an average of 40% (fig. S4). Moreover, after 20 days, the tumors in surviving cisplatin-treated mice began to grow, despite continued treatment with cisplatin. All the remaining cisplatin-treated mice died within 10 more days (Fig. 4A).

In contrast to cisplatin-treated mice, no loss of body weight was observed in peptide-treated mice (fig. S4), and the tumors continued to shrink until day 48, when there was no detectable luciferase signal in any of the mice (Fig. 4, A and B, and figs. S5 and S6). We continued to treat these mice for an additional 35 days (83 days in total), until the control-treated group displayed conditions associated with morbidity, such as ataxia and hunched posture. During this treatment time, the luciferase signal never reemerged in the peptide-treated mice, and gross examination of the mice revealed no metastatic lesions (Fig. 4, A and C). This was in stark contrast to the control-treated mice, which had multiple macrometastatic lesions visible on the surface of the liver and at the interface between the liver and pancreas (Fig. 4, C and D). At necropsy, all abdominal organs were examined grossly and the livers and spleens histologically (H&E). We were unable to identify any metastatic lesions in the psap peptide–treated mice, and the liver morphology did not appear abnormal (Fig. 4D).

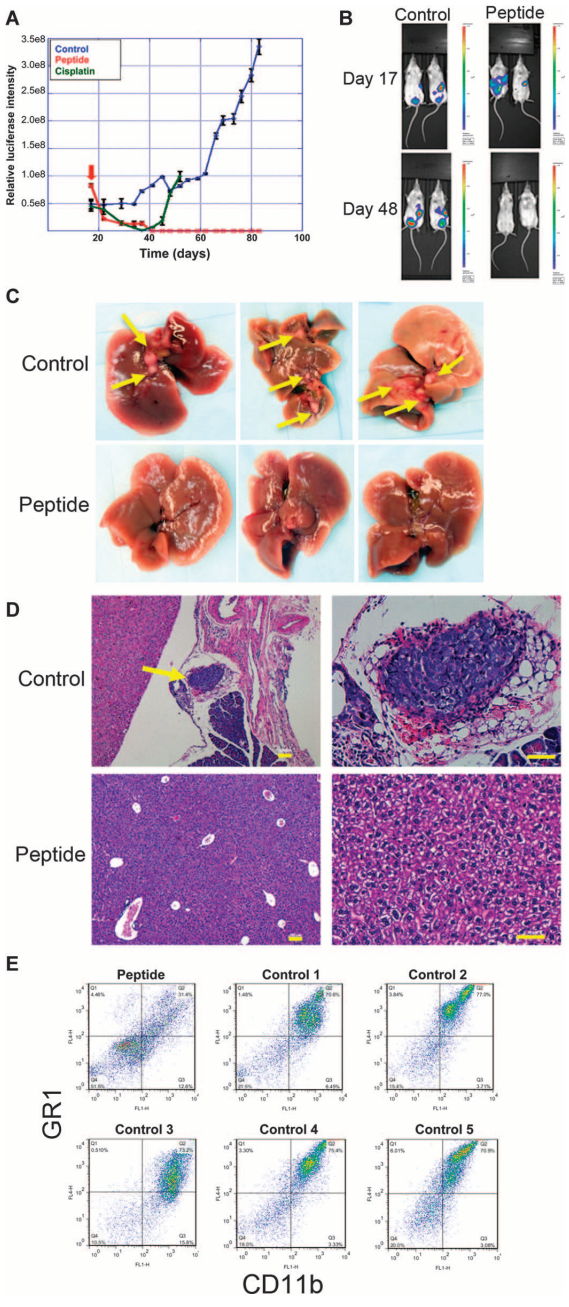

Fig. 4. Effects of a D-amino acid psap peptide on a PDX model of metastatic ovarian cancer. (**A**) Plot of relative luciferase intensity of metastatic ovarian PDX tumors that were treated with saline (Control), cisplatin (4 mg/kg every other day), and dWIP psap peptide (40 mg/kg daily). Red arrow indicates initiation of treatment ($n = 12$ mice per group) (mean ± SEM). (**B**) Luciferase imaging of two control-treated mice and two dWIP psap peptide–treated mice at day 17 (treatment day 0) and day 48 (treatment day 31). (**C**) Photographs of the livers of mice bearing metastatic ovarian PDX tumors treated with saline (Control) or dWIP psap peptide (Peptide) (arrows indicate metastases). (**D**) H&E staining of the liver of a mouse bearing metastatic ovarian PDX tumors treated with saline (Control) or dWIP psap peptide (Peptide) (arrow indicates metastatic lesions; scale bars, 100 μm). (**E**) FACS analysis of $GR1^+/Cd11b^+$ cells in the peritoneal fluid of control- and dWIP psap peptide (Peptide)–treated mice bearing metastatic ovarian PDX tumors after 48 days of treatment.

Finally, we sought to determine whether metastases in the peritoneal cavity recruited $CD11b^+/GR1^+$ bone marrow–derived cells, analogous to lung metastases (*6*). To that end, we collected ascites fluid from the peritoneal cavity of control-treated mice bearing DF14 metastases and fluid from the peritoneal cavity of psap peptide–treated mice that showed no signs of metastases. As was the case with mice bearing 1D8 tumors, the incidence of ascites fluid in peptide-treated mice (1 of 12) was lower than in control-treated mice (5 of 12). FACS analysis of the ascites fluid from these mice revealed that 71 to 77% of the cells in the peritoneal fluid of control-treated mice were $CD11b^+/GR1^+$ (Fig. 4E), whereas only 31.4% of the cells in the peritoneal fluid from the lone peptide-treated mouse that developed ascites were $CD11b^+/GR1^+$ (Fig. 4E). On the basis of these findings, we concluded that the psap peptide was able to stimulate regression of established metastases to the point where no detectable lesions could be found.

Cyclization further stabilizes the psap peptide and increases its activity

Although the results of the peptide treatment of the PDX model of ovarian cancer were very promising, we postulated that the stability and activity of the peptide could be further improved. We noted that the peptide that we derived from psap was located in a region of the protein that contained a 13–amino acid loop between two helices that was stabilized by a disulfide bond (*6*). We therefore synthesized a five–amino acid peptide that was cyclized via backbone (N-C) cyclization, in which the C-terminal lysine is linked via a peptide bond to the N-terminal aspartate. We then tested the activity of this peptide in vitro by evaluating its ability to stimulate TSP-1. We found that the cyclic peptide stimulated TSP-1 up to twofold greater than the D-amino acid linear peptide (Fig. 5A).

Cyclization of peptides is a process with the potential to increase stability by forcing peptides into a conformation that is not recognized by most naturally occurring proteases (*17*, *18*, *26*–*30*). We therefore compared the stability in human plasma of the cyclic psap-derived peptide to the linear D-amino acid peptide. We incubated both peptides in human plasma at 37°C for up to 24 hours and then tested the ability of the plasma/peptide mixture to stimulate TSP-1 in WI-38 fibroblasts. We measured the amount of secreted TSP-1 in lung fibroblasts after treatment with the peptide/plasma mixture by enzyme-linked immunosorbent assay (ELISA) and found that the stimulation of TSP-1 by the two peptides was roughly equivalent after up to 8 hours of incubation (Fig. 5B). However, after 24 hours of incubation in human plasma, the cyclic peptide retained greater than 70% of its TSP-1–stimulating activity, whereas the plasma that contained the linear peptide was no longer able to stimulate TSP-1 ($P = 0.003$, calculated by Student's *t* test) (Fig. 5B). Hence, we concluded that the cyclic peptide was more stable and active over a longer time than the linear D-amino acid peptide.

On the basis of these findings, we decided to test the efficacy of the cyclic peptide in the DF14 model. To better study the effects of the peptide on the metastatic lesions, we injected mice intraperitoneally with 1×10^6 cells and allowed the luciferase signal to reach 3.2×10^9 RLU. We then treated the mice with the cyclic peptide at a dose of 10 mg/kg per day (a lower dose than previously used, based on the increased in vitro activity and ex vivo stability/activity compared to the D1,3 peptide) for only 15 days to ensure that there would be sufficient tumor tissue to analyze. After only 15 days of treatment, the average luciferase signal in the peptide-treated mice decreased from 3.2×10^9 to 2.8×10^9, whereas the vehicle-treated tumors continued to grow (Fig. 5C). We then analyzed the omentum, which was the major site for metastatic lesions, by H&E staining and found that the metastatic lesions in the peptide-treated mice were ~2.3-fold smaller than those in the saline-treated mice ($P = 0.046$; as calculated by Student's *t* test) (Fig. 5, D and E).

We then stained the lesions in the omentum via immunohistochemistry and immunofluorescence for TSP-1, GR1, and TUNEL. Consistent with our previous observations, we found widespread TSP-1 expression in extracellular matrix, with virtually all of the $GR1^+$ cells in the metastatic microenvironment of psap peptide–treated mice staining positive for TSP-1 (Fig. 5F) (*6*). Conversely, TSP-1 expression was virtually undetectable in the microenvironment of metastatic lesions of control-treated mice (Fig. 5F). On the basis of the induced expression of TSP-1 and the observation that all of the patient-derived ovarian cancer cells that we evaluated express CD36 (Fig. 1C), we sought to determine whether the TSP-1 expression in the metastatic microenvironment was inducing apoptosis in the tumor cells, as observed in vitro (Fig. 1E). TUNEL staining revealed that the metastatic lesions in the peptide-treated mice contained a significantly greater percentage of apoptotic cells compared to control (saline)–treated tumors (59% versus 11.4%) ($P < 0.0001$, Fisher's exact test) (Fig. 5, G and H).

Metastatic HGSOC tumors express less psap but more CD36 than primary tumors

Having demonstrated the activity of the psap peptides against tumors formed by patient-derived ovarian cancer cells, which all expressed CD36, we sought to determine how prevalent CD36 expression was in human ovarian cancer patients, and thus how widely applicable a potential psap-based therapeutic agent would be for this disease. We also postulated, on the basis of its biological activity, that psap expression should decrease as tumors progress to the metastatic stage. Accordingly, we used a previously described high-density tissue microarray (TMA) composed of 134 cases with metastatic HGSOC and normal tissue from 46 patients (stage III or IV) (*31*). We then stained the tissue for CD36 and psap expression and scored the intensity using the staining index (SI) method (*6*). We found that 61% of normal tissue expressed CD36 with an average SI of 2.39 (of a possible maximum score of 9) (Fig. 6, A and B, fig. S7, and Table 1). Analysis of 134 primary ovarian tumors revealed that 97% (130 of 134) of tumors stained positive for CD36 with an average SI of 5.32, which was significantly higher than that of normal tissue ($P < 0.0001$; calculated by Wilcoxon-Mann-Whitney) (Fig. 6, A and B, and Table 1). When we examined 121 visceral metastases from the 134 patients, we found that 97% (117 of 121) of the metastatic lesions stained positive for CD36 with an average SI of 6.61, which was significantly higher than that of primary serous ovarian tumors ($P = 0.0003$; calculated by Mann-Whitney *U* test) (Fig. 6, A and B, and Table 1). Finally, we observed that 100% of lymph node metastases (13 of 13) stained positive for CD36 with an average SI of 6.69, which did not differ statistically from that of primary tumors because of the small sample size ($P = 0.1006$ by Mann-Whitney *U* test) (Fig. 6, A and B, and Table 1).

We then turned our attention to the expression of psap in human ovarian cancer patients with the expectation that it should decrease with tumor progression based on its mechanism of action. When we examined psap expression in the ovarian cancer TMA samples, we found that normal ovaries expressed relatively low amounts of psap with an average SI of 4.29 (Fig. 6, C and D, and Table 2). Primary

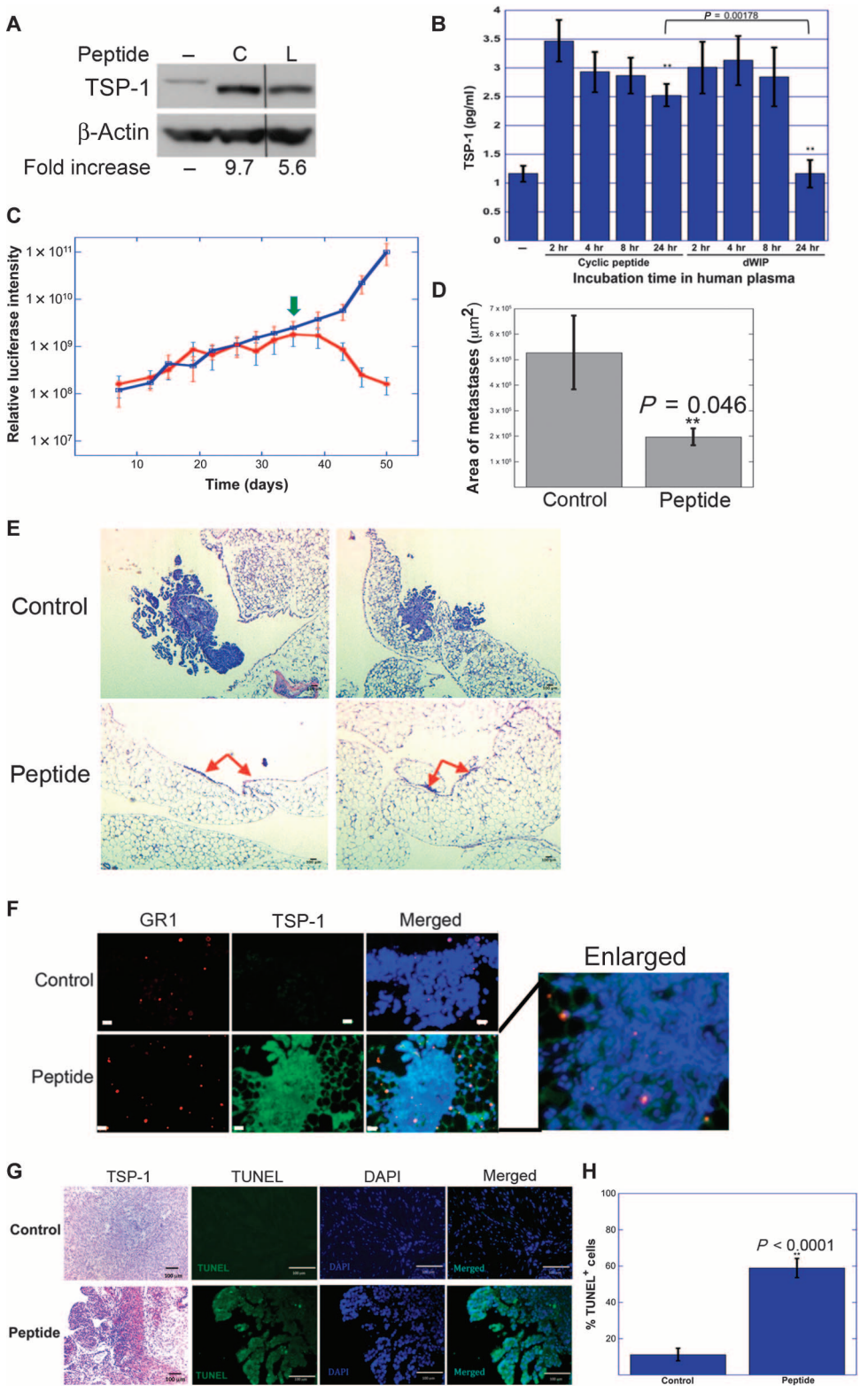

Fig. 5. Effects of a cyclic psap peptide on TSP-1 expression and a PDX model of metastatic ovarian cancer. (**A**) Western blot of TSP-1 and β-actin in WI-38 lung fibroblasts that were untreated (–) or treated with cyclic DWLPK psap peptide (C) or D1,3 psap peptide (L) (line represents digital excision of bands not relevant to this study). (**B**) ELISA of TSP-1 expression in WI-38 lung fibroblasts that were untreated (–) or treated with dWlP psap peptide (D1,3) or with cyclic DWLPK psap peptide after up to 24 hours of incubation in human plasma at 37°C (*P* values calculated by ANOVA) (mean ± SEM). (**C**) Plot of relative luciferase intensity of metastatic ovarian PDX tumors that were treated with saline (blue line) or cyclic DWLPK psap peptide (red line) (10 mg/kg daily). Green arrow indicates onset of treatment. (**D**) Plot of average area of metastatic lesions in saline (Control)– and cyclic DWLPK psap peptide (Peptide)–treated mice. (*P* values were calculated by ANOVA) (error bars indicate means ± SEM). (**E**) H&E staining of metastatic lesions (indicated by red arrows) in the omentum of mice treated with vehicle (saline; Control) or cyclic psap peptide (Peptide) (scale bar, 100 μm). (**F**) Immunofluorescence staining of GR1 and TSP-1 expression in metastatic lesions of control-treated mice and cyclic DWLPK psap peptide (Peptide)–treated mice (scale bar, 50 μm; enlarged panel, fourfold enlarged). (**G**) Immunohistochemistry (leftmost panels) of TSP-1 expression (scale bar, 100 μm), immunofluorescence staining of TUNEL (green) and DAPI (blue), and merged images of TUNEL and DAPI for metastatic lesions in control- and cyclic DWLPK psap peptide (Peptide)–treated mice (scale bar, 100 μm). (**H**) Plot of %TUNEL-positive cells in saline (Control)– and psap peptide (Peptide)–treated tumors (*P* values were calculated by Fisher's exact test).

ovarian tumors expressed significantly more psap than normal tissue, with an average SI of 5.17 ($P = 0.0037$; calculated by Mann-Whitney *U* test) (Fig. 6, C and D, and Table 2). However, when we examined the expression of PSAP in visceral and lymph node metastases, we found that it was significantly lower than in primary tumors, with average SIs of 4.14 and 4.07, respectively ($P < 0.0001$; calculated by Mann-Whitney *U* test) (Fig. 6, C and D, and Table 2). Thus, when taken together, these findings demonstrate that CD36 expression is increased

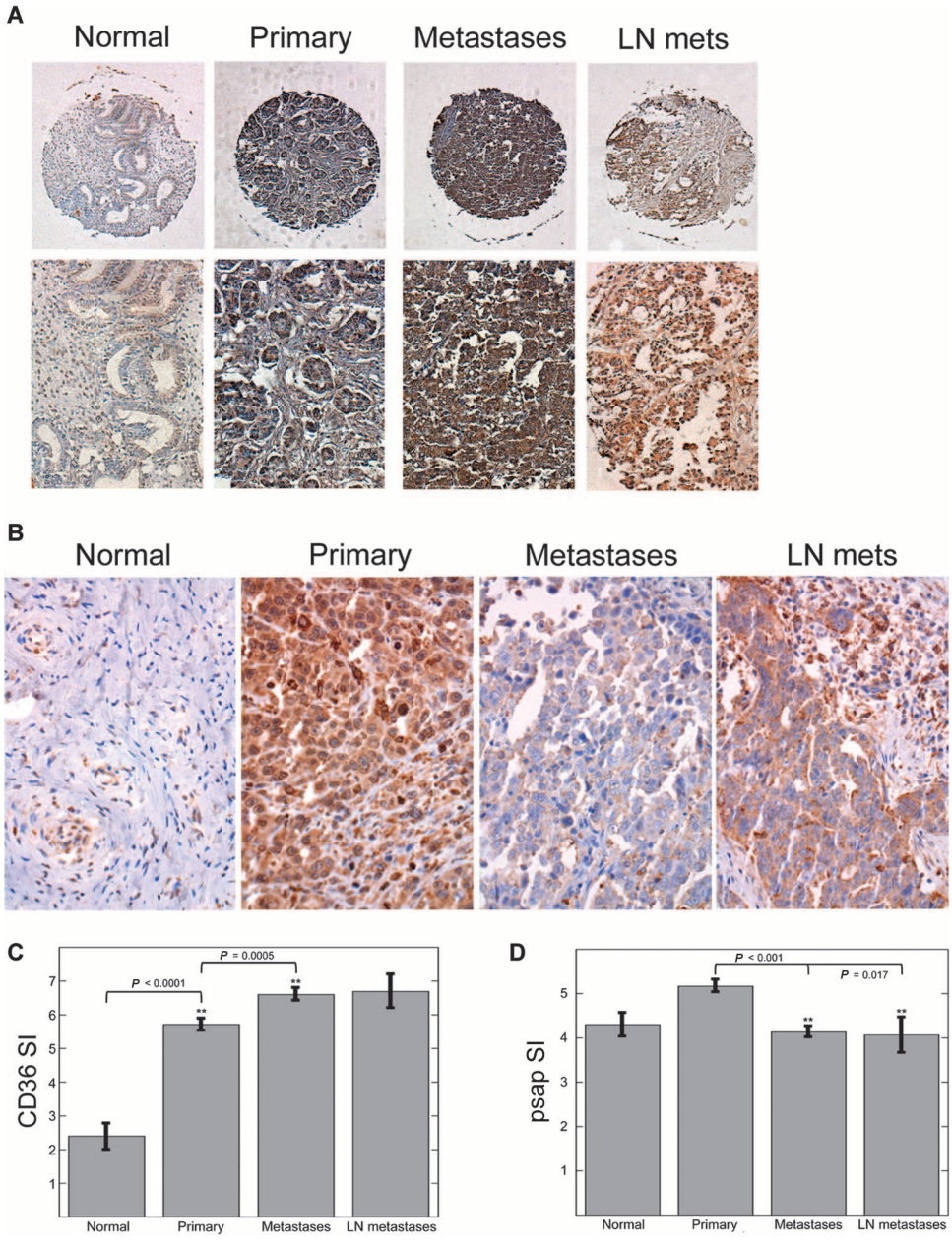

Fig. 6. Expression of CD36 and psap in a TMA of human ovarian cancer patients. (**A**) Expression of CD36 in a tumor TMA compiled from normal tissue, primary human ovarian tumors, human ovarian cancer visceral metastases (metastases), and human ovarian cancer lymph node metastases (LN mets) (black scale bars, 200 μm; yellow scale bars, 50 μm). (**B**) Plot of CD36 SIs for normal human ovarian and endometrial tissue, primary human ovarian tumors, human ovarian cancer metastases, and human ovarian cancer lymph node metastases (*P* values were determined by Wilcoxon-Mann-Whitney analysis) (mean ± SEM). (**C**) Expression of psap in a tumor TMA compiled from normal tissue, primary human ovarian tumors, human ovarian cancer visceral metastases (metastases), and human ovarian cancer lymph node metastases (LN mets) (scale bars, 50 μm). (**D**) Plot of psap SIs for normal human ovarian and endometrial tissue, primary human ovarian tumors, human ovarian cancer metastases, and human ovarian cancer lymph node metastases (*P* values were determined by Wilcoxon-Mann-Whitney analysis) (mean ± SEM).

in primary ovarian tumors compared to normal tissue and is further increased in metastatic lesions compared to primary tumors, whereas psap expression decreases with tumor progression. These findings suggest that metastatic ovarian tumors repress psap expression but retain CD36, which supports the hypothesis that ovarian cancer could be effectively treated with a psap-derived therapy.

DISCUSSION

Ovarian cancer is one of the most lethal malignancies, with a 5-year survival rate of <10% for advanced-stage (stage III/IV) patients (*1*). Although platinum-based therapies in combination with taxanes display efficacy in patients with early-stage disease, most patients eventually develop resistance. For these patients, there are no approved therapies that appreciably extend their survival. Accordingly, we set out to develop a therapeutic agent to treat advanced-stage HGSOC.

Through an analysis of human ovarian cancer cell lines isolated directly from patient ascites, we found that all tested cell lines express CD36, the receptor for TSP-1, which is the downstream target of psap and the psap peptide in bone marrow–derived cells. We also demonstrated that recombinant TSP-1 induces apoptosis in these CD36-expressing serous ovarian cancer cells. On the basis of these findings, we hypothesized that a peptide derived from psap, which stimulates the expression of TSP-1 in bone marrow–derived monocytes (*6*, *7*), could be effective in treating high-grade serous ovarian tumors.

Here, we demonstrated that the in vitro proapoptotic effect of TSP-1 on ovarian cancer cells could be recapitulated in both a syngeneic and a PDX model of ovarian cancer using two different psap-derived peptides. The induced expression of TSP-1 in these models resulted in apoptosis in the tumor cells and regression of established metastases.

In addition to demonstrating that induction of TSP-1 can induce the regression of ovarian tumors, we also delineated the development process of a cyclic peptide derived from psap, which has greater activity and stability than the native peptide. Specifically, we demonstrated that incorporation of D-amino acids at the first and third residues of the native linear peptide increases in vivo activity. We then further modified the peptide to make it more drug-like by cyclizing a five–amino acid peptide via backbone N-C cyclization. The cyclic peptide displayed even greater in vivo activity than the D-amino acid linear peptide. Moreover, we demonstrated that both modified peptides can promote regression

Table 1. CD36 expression in human HGSOC patient TMA

	SI	% Positive samples	% Samples with SI >6	*P*
Normal	2.39	61% (28/46)	28.3	
Primary serous EOC	5.38	97% (130/134)	79.9	<0.0001
Visceral metastases	6.61	97% (117/121)	91.7	0.0003
Lymph node metastases	6.69	100% (13/13)	92.3	0.1006

Table 2. Psap expression in human HGSOC patient TMA

	Psap SI	*P*
Normal	4.3	—
Primary serous EOC	5.17	0.0037
Visceral metastases	4.14	<0.001
Lymph node metastases	4.07	0.017

of established metastases in a PDX model of ovarian cancer. The cells used in this PDX model were derived from patients resistant to platinum, the most common first-line treatment for ovarian cancer. Treatment with either the D1,3 or cyclic psap peptide resulted in no observed toxicity, either grossly by way of body weight or hair loss or histologically as measured by liver morphology.

Our results demonstrate that the psap peptide is capable of inhibiting ovarian cancer progression via three distinct mechanisms, all mediated by the induction of TSP-1. The first is via direct cell killing mediated by downstream signaling from CD36 triggered by TSP-1 (*12*). The second is via the widely established antiangiogenic activity of TSP-1 (*8*). The third is via recruitment of macrophages, which is consistent with TSP-1 binding to its other cell surface receptor, CD47, to block the "do not eat me" signal mediated by CD47 binding to SIRPα on macrophages (*32*, *33*).

Finally, an analysis of tumor tissue from 134 patients with serous ovarian cancer revealed that 97% of the tumors expressed CD36. CD36 expression was not only maintained in metastatic lesions but also actually increased with tumor progression. In addition to being a receptor for TSP-1, CD36 is also a fatty acid translocase (*34*, *35*). In this context, it should be noted that ovarian cancer has a propensity for metastasizing to the omentum, a fatty structure in the lower abdomen (*36*). Together, these findings suggest that there may be a causative relationship between CD36 expression and ovarian cancer metastasis. In this scenario, the selective pressure to maintain CD36 expression may prevent the development of resistance to a psap/TSP-1–based therapeutic agent, because loss of CD36 would decrease the tumor's ability to use lipids as a source of energy.

One limitation of this study is that, although we were able to establish that virtually all serous ovarian cancer cells that we analyzed express CD36 and that rhTSP-1 was able to induce apoptosis in a subset of these cells in a CD36-dependent manner, we were only able to test the efficacy of the PSAP peptides in two animal models. Therefore, although we can predict that the PSAP peptide could have potent efficacy against ovarian cancer in patients, many more models will need to be tested before this prediction can be validated.

The findings that we present here suggest that a psap-based therapeutic agent could have efficacy for the vast majority of ovarian cancer patients, given its mechanism of action and the prevalence of CD36 expression in the tumor cells of these patients. The fact that the cyclic psap peptide has efficacy at a dose that translates to <1 mg/kg (*37*) for human patients and has drug-like stability suggests that, with continued preclinical development, it could be a viable therapeutic agent that may be able to extend the lives and improve the quality of life for patients with HGSOC.

MATERIALS AND METHODS

Study design

The number of animals for studies was calculated using Power calculations with an f^2 of 0.35 and a desired *P* value of 0.05, allowing us to use a minimum of eight animals per group. Animal experiments were ended when mice in any group met criteria for euthanasia as defined by the Boston Children's Hospital Institutional Animal Care and Use Committee. The objective of this study was to determine whether stimulation of TSP-1 in the tumor microenvironment by peptides derived from psap would inhibit or reverse the growth of primary ovarian tumors and metastases expressing CD36, a receptor for TSP-1 that mediates its apoptotic activity. Animals were assigned to study groups based on the luciferase intensities at the onset of treatment such that each group had average luciferase intensities that were as similar as possible. Where more than one treatment was used, the treatments were keyed, and dosing was performed in a blinded manner. At the end point of the experiment, the study was unblinded by revealing the key to the person analyzing the data. All in vitro experiments were performed in triplicate with a minimum of five independent replicates. Animal studies were performed a minimum of one time with studies powered accordingly.

Research objective

The objective of this study was to determine whether stimulation of TSP-1 in the tumor microenvironment by peptides derived from psap would inhibit or reverse the growth of primary ovarian tumors and metastases expressing CD36, a receptor for TSP-1 that mediates its apoptotic activity.

Research subjects

The subjects of the research conducted in this study were C.B-17 SCID mice and C57BL6/J mice. We also used patient-derived ovarian cancer cells that were treated in culture with different agents.

Experimental design

We conducted a controlled animal study to test the effects of two peptides derived from psap on the growth and survival of metastatic colonies formed by patient-derived ovarian cancer cells in the peritoneal cavity of SCID mice. The mice were treated with two peptides, a

four–amino acid linear peptide with D-amino acids incorporated in the first and third residues and a cyclic five–amino acid peptide. The mice were also treated with cisplatin to compare the efficacy and safety of the peptides with a commonly used chemotherapeutic agent. The control treatment for the mice was saline, the vehicle used to deliver the peptides and cisplatin. Tumors were monitored by in vivo bioluminescent imaging, because the cells were labeled with luciferase. Body weight was also recorded throughout the course of treatment.

Animal tumor models

Ovarian cancer PDX model. For the ovarian cancer PDX model, 8-week-old female SCID mice ($n = 12$ per group) were injected with 1×10^6 DF14 cells, which were derived from patient ascites and expressed firefly luciferase, into the peritoneal cavity. The growth of metastatic colonies in the mice was monitored by a Xenogen IVIS-200 system (Xenogen) twice per week. The mice were treated when the average intensity of the luciferase signal was between 0.5 and 1×10^8 RLU. The dose for the D-amino acid peptide (>95% purity) (AnaSpec) was 40 mg/kg per day, and the dose for *cis*-diamineplatinum(II) dichloride (cisplatin, Sigma-Aldrich) was 4 mg/kg every other day. Both drugs were administered by intraperitoneal injection.

To better study the effects of the cyclic peptide (>95% purity) (AnaSpec), 8-week-old female SCID mice ($n = 16$ mice per group) were injected with 1×10^6 DF14 cells into the peritoneal cavity. The growth of metastatic colonies in the mice was monitored by a Xenogen IVIS system twice per week. Mice were treated when the average intensity of the luciferase signal reached 9×10^9 RLU. The dose for the cyclic peptide was 10 mg/kg per day, administered by intraperitoneal injection. Statistical significance for differences in luciferase intensity, body weight, and tumor area was determined by ANOVA.

Statistical analysis

Differences in cell survival, proliferation, and secretion of TSP-1 measured by ELISA were evaluated for statistical significance by ANOVA (KaleidaGraph, Synergy Software). Differences in the area of metastatic lesions between treated and untreated mice were evaluated for statistical significance by Student's t test (KaleidaGraph, Synergy Software). Differences in the fraction of TUNEL-positive cells between tumors treated with saline and tumors treated with the cyclic psap peptide were evaluated for statistical significance by χ^2 and Fisher's exact test. Differences in SIs of ovarian cancer patient tumor microarrays were evaluated for statistical significance by Wilcoxon-Mann-Whitney analysis (KaleidaGraph, Synergy Software). For all analyses, P values <0.05 were considered statistically significant. All tests were two-tailed. Original data for individual mice are provided in table S2.

SUPPLEMENTARY MATERIALS

www.sciencetranslationalmedicine.org/cgi/content/full/8/329/329ra34/DC1
Materials and Methods
Fig. S1. Expression of CD36 in patient-derived ovarian cancer cells.
Fig. S2. FACS analysis of rhTSP-1 effects on ovarian cancer cell apoptosis.
Fig. S3. Effects of CD36 blocking antibody on rhTSP-1 induction of ovarian cancer cell apoptosis.
Fig. S4. Body weight tracking of mice bearing patient-derived ovarian cancer metastases.
Fig. S5. Bioluminescent imaging of peptide-treated patient-derived ovarian cancer metastases.
Fig. S6. Bioluminescent imaging of control-treated patient-derived ovarian cancer metastases.
Fig. S7. CD36 staining of ovarian cancer patient TMA.
Table S1. Characterization of platinum sensitivity of patient-derived ovarian cancer cells.
Table S2. Original data (provided as an Excel file).
References (*38*, *39*)

REFERENCES AND NOTES

1. A. M. Karst, R. Drapkin, Ovarian cancer pathogenesis: A model in evolution. *J. Oncol.* **2010**, 932371 (2010).
2. L. Dubeau, R. Drapkin, Coming into focus: The nonovarian origins of ovarian cancer. *Ann. Oncol.* **24** (Suppl. 8), viii28–viii35 (2013).
3. B. W. Stewart, C. P. Wild, *World Cancer Report 2014* (WHO Press, Geneva, 2014).
4. K. Matsuo, V. K. Bond, M. L. Eno, D. D. Im, N. B. Rosenshein, Low drug resistance to both platinum and taxane chemotherapy on an in vitro drug resistance assay predicts improved survival in patients with advanced epithelial ovarian, fallopian and peritoneal cancer. *Int. J. Cancer* **125**, 2721–2727 (2009).
5. K. Matsuo, M. L. Eno, D. D. Im, N. B. Rosenshein, A. K. Sood, Clinical relevance of extent of extreme drug resistance in epithelial ovarian carcinoma. *Gynecol. Oncol.* **116**, 61–65 (2010).
6. R. Catena, N. Bhattacharya, T. El Rayes, S. Wang, H. Choi, D. Gao, S. Ryu, N. Joshi, D. Bielenberg, S. B. Lee, S. A. Haukaas, K. Gravdal, O. J. Halvorsen, L. A. Akslen, R. S. Watnick, V. Mittal, Bone marrow–derived Gr1$^+$ cells can generate a metastasis-resistant microenvironment via induced secretion of thrombospondin-1. *Cancer Discov.* **3**, 578–589 (2013).
7. S.-Y. Kang, O. J. Halvorsen, K. Gravdal, N. Bhattacharya, J. M. Lee, N. W. Liu, B. T. Johnston, A. B. Johnston, S. A. Haukaas, K. Aamodt, S. Yoo, L. A. Akslen, R. S. Watnick, Prosaposin inhibits tumor metastasis via paracrine and endocrine stimulation of stromal p53 and Tsp-1. *Proc. Natl. Acad. Sci. U.S.A.* **106**, 12115–12120 (2009).
8. D. J. Good, P. J. Polverini, F. Rastinejad, M. M. Le Beau, R. S. Lemons, W. A. Frazier, N. P. Bouck, A tumor suppressor-dependent inhibitor of angiogenesis is immunologically and functionally indistinguishable from a fragment of thrombospondin. *Proc. Natl. Acad. Sci. U.S.A.* **87**, 6624–6628 (1990).
9. J. Lawler, W.-M. Miao, M. Duquette, N. Bouck, R. T. Bronson, R. O. Hynes, Thrombospondin-1 gene expression affects survival and tumor spectrum of p53-deficient mice. *Am. J. Pathol.* **159**, 1949–1956 (2001).
10. W.-M. Miao, W. Lin Seng, M. Duquette, P. Lawler, C. Laus, J. Lawler, Thrombospondin-1 type 1 repeat recombinant proteins inhibit tumor growth through transforming growth factor-β-dependent and -independent mechanisms. *Cancer Res.* **61**, 7830–7839 (2001).
11. R. N. Kaplan, R. D. Riba, S. Zacharoulis, A. H. Bramley, L. Vincent, C. Costa, D. D. MacDonald, D. K. Jin, K. Shido, S. A. Kerns, Z. Zhu, D. Hicklin, Y. Wu, J. L. Port, N. Altorki, E. R. Port, D. Ruggero, S. V. Shmelkov, K. K. Jensen, S. Rafii, D. Lyden, VEGFR1-positive haematopoietic bone marrow progenitors initiate the pre-metastatic niche. *Nature* **438**, 820–827 (2005).
12. D. W. Dawson, S. F.A. Pearce, R. Zhong, R. L. Silverstein, W. A. Frazier, N. P. Bouck, CD36 mediates the in vitro inhibitory effects of thrombospondin-1 on endothelial cells. *J. Cell Biol.* **138**, 707–717 (1997).
13. S. Russell, M. Duquette, J. Liu, R. Drapkin, J. Lawler, J. Petrik, Combined therapy with thrombospondin-1 type I repeats (3TSR) and chemotherapy induces regression and significantly improves survival in a preclinical model of advanced stage epithelial ovarian cancer. *FASEB J.* **29**, 576–588 (2014).
14. V. Bobde, Y. U. Sasidhar, S. Durani, Harnessing D-amino acids for peptide motif designs. synthesis and solution conformation of Boc-D-Glu-Ala-Gly-Lys-NHMe and Boc-L-Glu-Ala-Gly-Lys-NHMe. *Int. J. Pept. Protein Res.* **43**, 209–218 (1994).
15. M. Coltrera, M. Rosenblatt, J. T. Potts Jr., Analogues of parathyroid hormone containing D-amino acids: Evaluation of biological activity and stability. *Biochemistry* **19**, 4380–4385 (1980).
16. A. S. Dutta, M. B. Giles, Polypeptides. Part XIV. A comparative study of the stability towards enzymes of model tripeptides containing α-aza-amino-acids, L-amino-acids, and D-amino-acids. *J. Chem. Soc. Perkin 1*, 244–248 (1976).
17. A. G. Lamont, M. F. Powell, S. M. Colón, C. Miles, H. M. Grey, A. Sette, The use of peptide analogs with improved stability and MHC binding capacity to inhibit antigen presentation in vitro and in vivo. *J. Immunol.* **144**, 2493–2498 (1990).
18. M. F. Powell, T. Stewart, L. Otvos Jr., L. Urge, F. C. A. Gaeta, A. Sette, T. Arrhenius, D. Thomson, K. Soda, S. M. Colon, Peptide stability in drug development. II. Effect of single amino acid substitution and glycosylation on peptide reactivity in human serum. *Pharm. Res.* **10**, 1268–1273 (1993).
19. J. Greenaway, J. Henkin, J. Lawler, R. Moorehead, J. Petrik, ABT-510 induces tumor cell apoptosis and inhibits ovarian tumor growth in an orthotopic, syngeneic model of epithelial ovarian cancer. *Mol. Cancer Ther.* **8**, 64–74 (2009).
20. J. J. Petrik, P. A. Gentry, J.-J. Feige, J. LaMarre, Expression and localization of thrombospondin-1 and -2 and their cell-surface receptor, CD36, during rat follicular development and formation of the corpus luteum. *Biol. Reprod.* **67**, 1522–1531 (2002).
21. K. Li, M. Yang, P. M. P. Yuen, K. W. Chik, C. K. Li, M. Ming, K. Shing, H. K. B. Lam, T. F. Fok, Thrombospondin-1 induces apoptosis in primary leukemia and cell lines mediated by CD36 and caspase-3. *Int. J. Mol. Med.* **12**, 995–1001 (2003).

22. N. Campbell, J. Greenaway, J. Henkin, J. Petrik, ABT-898 induces tumor regression and prolongs survival in a mouse model of epithelial ovarian cancer. *Mol. Cancer Ther.* **10**, 1876–1885 (2011).
23. G. Martin-Manso, S. Galli, L. A. Ridnour, M. Tsokos, D. A. Wink, D. D. Roberts, Thrombospondin 1 promotes tumor macrophage recruitment and enhances tumor cell cytotoxicity of differentiated U937 cells. *Cancer Res.* **68**, 7090–7099 (2008).
24. A. Clauss, V. Ng, J. Liu, H. Piao, M. Russo, N. Vena, Q. Sheng, M. S Hirsch, T. Bonome, U. Matulonis, A. H Ligon, M. J Birrer, R. Drapkin, Overexpression of elafin in ovarian carcinoma is driven by genomic gains and activation of the nuclear factor κB pathway and is associated with poor overall survival. *Neoplasia* **12**, 161–172 (2010).
25. S. Ghamande, B. L. Hylander, E. Oflazoglu, S. Lele, W. Fanslow, E. A. Repasky, Recombinant CD40 ligand therapy has significant antitumor effects on CD40-positive ovarian tumor xenografts grown in SCID mice and demonstrates an augmented effect with cisplatin. *Cancer Res.* **61**, 7556–7562 (2001).
26. S. J. Bogdanowich-Knipp, S. Chakrabarti, T. D. Williams, R. K. Dillman, T. J. Siahaan, Solution stability of linear vs. cyclic RGD peptides. *J. Pept. Res.* **53**, 530–541 (1999).
27. H. Iwai, A. Plückthun, Circular β-lactamase: Stability enhancement by cyclizing the backbone. *FEBS Lett.* **459**, 166–172 (1999).
28. A. X. Ji, M. Bodanszky, Cyclization studies with a model pentapeptide. *Int. J. Pept. Protein Res.* **22**, 590–596 (1983).
29. J. Møss, H. Bundgaard, Kinetics and mechanism of the facile cyclization of histidylprolineamide to cyclo (His-Pro) in aqueous solution and the competitive influence of human plasma. *J. Pharm. Pharmacol.* **42**, 7–12 (1990).
30. J. Samanen, F. Ali, T. Romoff, R. Calvo, E. Sorenson, J. Vasko, B. Storer, D. Berry, D. Bennett, Development of a small RGD peptide fibrinogen receptor antagonist with potent antiaggregatory activity in vitro. *J. Med. Chem.* **34**, 3114–3125 (1991).
31. J. F. Liu, M. S. Hirsch, H. Lee, U. A. Matulonis, Prognosis and hormone receptor status in older and younger patients with advanced-stage papillary serous ovarian carcinoma. *Gynecol. Oncol.* **115**, 401–406 (2009).
32. P. Burger, P. Hilarius-Stokman, D. de Korte, T. K. van den Berg, R. van Bruggen, CD47 functions as a molecular switch for erythrocyte phagocytosis. *Blood* **119**, 5512–5521 (2012).
33. A. Saumet, M. B. Slimane, M. Lanotte, J. Lawler, V. Dubernard, Type 3 repeat/C-terminal domain of thrombospondin-1 triggers caspase-independent cell death through CD47/αvβ3 in promyelocytic leukemia NB4 cells. *Blood* **106**, 658–667 (2005).
34. N. A. Abumrad, M. R. el-Maghrabi, E. Z. Amri, E. Lopez, P. A. Grimaldi, Cloning of a rat adipocyte membrane protein implicated in binding or transport of long-chain fatty acids that is induced during preadipocyte differentiation. Homology with human CD36. *J. Biol. Chem.* **268**, 17665–17668 (1993).
35. C. M. Harmon, N. A. Abumrad, Binding of sulfosuccinimidyl fatty acids to adipocyte membrane proteins: Isolation and amino-terminal sequence of an 88-kD protein implicated in transport of long-chain fatty acids. *J. Membr. Biol.* **133**, 43–49 (1993).
36. S. Pradeep, S. W. Kim, S. Y. Wu, M. Nishimura, P. Chaluvally-Raghavan, T. Miyake, C. V. Pecot, S.-J. Kim, H. J. Choi, F. Z. Bischoff, J. A. Mayer, L. Huang, A. M. Nick, C. S. Hall, C. Rodriguez-Aguayo, B. Zand, H. J. Dalton, T. Arumugam, H. J. Lee, H. D. Han, M. S. Cho, R. Rupaimoole, L. S. Mangala, V. Sehgal, S. C. Oh, J. Liu, J.-S. Lee, R. L. Coleman, P. Ram, G. Lopez-Berestein, I. J. Fidler, A. K. Sood, Hematogenous metastasis of ovarian cancer: Rethinking mode of spread. *Cancer Cell* **26**, 77–91 (2014).
37. S. Reagan-Shaw, M. Nihal, N. Ahmad, Dose translation from animal to human studies revisited. *FASEB J.* **22**, 659–661 (2008).
38. C. A. Pettaway, S. Pathak, G. Greene, E. Ramirez, M. R. Wilson, J. J. Killion, I. J. Fidler, Selection of highly metastatic variants of different human prostatic carcinomas using orthotopic implantation in nude mice. *Clin. Cancer Res.* **2**, 1627–1636 (1996).
39. R. Sanches, M. Kuiper, F. Penault-Llorca, B. Aunoble, C. D'Incan, Y.-J. Bignon, Antitumoral effect of interleukin-12-secreting fibroblasts in a mouse model of ovarian cancer: Implications for the use of ovarian cancer biopsy-derived fibroblasts as a vehicle for regional gene therapy. *Cancer Gene Ther.* **7**, 707–720 (2000).

Acknowledgments: We thank B. Zetter for the critical reading of the manuscript. We thank J. Lawler and A. Kung for valuable reagents. We thank M. Rogers, D. Panigrahy, L. Cryan, Y. Xu, and J. Styles for helpful suggestions and G. L. Hallseth and B. Nordanger for technical support. **Funding:** This study was supported by NIH grant CA135417 to V.M. and R.S.W. and by grants from the Norwegian Cancer Society and the Norwegian Research Council to L.A.A. R.D. was supported by NIH P50-CA083636, NIH U01-CA152990, NIH R21-CA156021, the Dr. Miriam and Sheldon G. Adelson Medical Research Foundation, and the Honorable Tina Brozman Foundation. This study was also partially supported by the Cornell Center on the Microenvironment and Metastasis through award no. U54CA143876 from the National Cancer Institute and Robert I. Goldman Foundation to V.M. and by the Elsa U. Pardee Foundation and Boston Children's Hospital Technology Development Fund to R.S.W. D.R.B. and R.S.W. were supported by the Vascular Biology Program at Boston Children's Hospital. J.F.L. received funding from the Ovarian Cancer Research Fund and Pallotta Investigator Award. **Author contributions:** S.W.: Designed and performed experiments, analyzed data, and participated in writing the manuscript. A.B.: Designed and performed experiments, analyzed data, and participated in writing the manuscript. T.E.R.: Designed experiments, analyzed data, and participated in writing the manuscript. J.F.L.: Performed experiments, analyzed data, and participated in writing the manuscript. M.S.H.: Performed experiments and analyzed data. K.G.: Designed experiments and analyzed data. S.P.: Performed experiments. D.R.B.: Designed and performed experiments and analyzed data. L.A.A.: Designed experiments, analyzed data, and participated in writing the manuscript. R.D.: Designed experiments, analyzed data, and participated in writing the manuscript. V.M.: Designed experiments, analyzed data, and participated in writing the manuscript. R.S.W.: Designed and performed experiments, analyzed data, and participated in writing the manuscript. **Competing interests:** R.S.W. is the scientific founder of, and has equity in, Vigeo Therapeutics Inc., which has licensed the patents covering the psap peptides from Boston Children's Hospital. **Data and materials availability:** Peptides and cell lines will be made available to academic researchers with material transfer agreements.

Submitted 1 October 2015
Accepted 4 February 2016
Published 9 March 2016
10.1126/scitranslmed.aad5653

Citation: S. Wang, A. Blois, T. El Rayes, J. F. Liu, M. S. Hirsch, K. Gravdal, S. Palakurthi, D. R. Bielenberg, L. A. Akslen, R. Drapkin, V. Mittal, R. S. Watnick, Development of a prosaposin-derived therapeutic cyclic peptide that targets ovarian cancer via the tumor microenvironment. *Sci. Transl. Med.* **8**, 329ra34 (2016).

Science Translational Medicine
AAAS

Development of a prosaposin-derived therapeutic cyclic peptide that targets ovarian cancer via the tumor microenvironment

Suming Wang, Anna Blois, Tina El Rayes, Joyce F. Liu, Michelle S. Hirsch, Karsten Gravdal, Sangeetha Palakurthi, Diane R. Bielenberg, Lars A. Akslen, Ronny Drapkin, Vivek Mittal and Randolph S. Watnick (March 9, 2016)

Science Translational Medicine **8** (329), 329ra34. [doi: 10.1126/scitranslmed.aad5653]

Editor's Summary

Running rings around ovarian cancer

Although approved drugs for ovarian cancer are available, this remains a difficult disease to overcome, and most ovarian cancer patients cannot be successfully treated, particularly in the setting of advanced disease. Wang *et al*. determined that prosaposin, a naturally occurring protein with antimetastatic properties, can promote regression of ovarian cancer because of its effects on thrombospondin, another antitumorigenic protein, which targets a receptor called CD36. The authors generated a cyclic peptide modeled on the active site of prosaposin and showed that the new peptide is very effective in treating mice with patient-derived xenografts of metastatic ovarian cancer, suggesting that this peptide is a candidate for future testing in human patients.

Science Translational Medicine (print ISSN 1946-6234; online ISSN 1946-6242) is published weekly, except the last week in December, by the American Association for the Advancement of Science, 1200 New York Avenue, NW, Washington, DC 20005.